DOI: 10.1038/ncb2916

nature cell biology

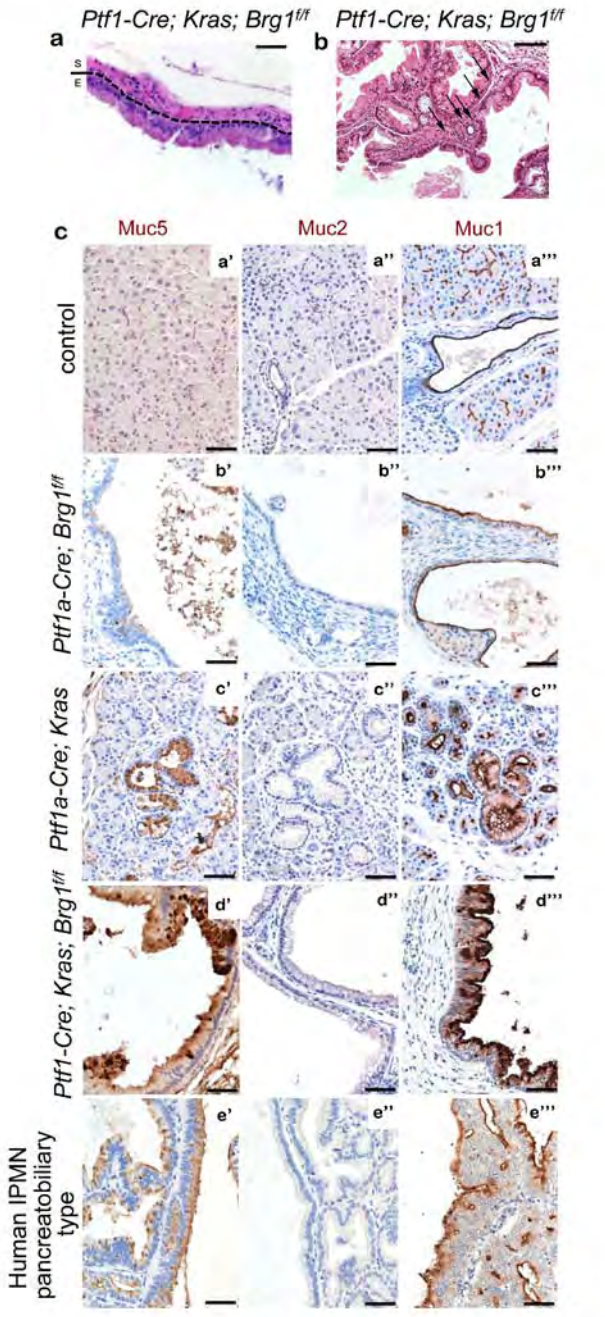

Supplementary Figure 1 Cystic lesions in *Ptf1a-Cre; Kras^{G12D}; Brg1$^{f/f}$* pancreata are marked by thin stroma and are reminiscent of human pancreatobiliary IPMN. (**a**) Representative H&E staining of a cystic lesion in *Ptf1a-Cre; Kras^{G12D}; Brg1$^{f/f}$* pancreata reveals thin underlying stroma (S = stroma, E = epithelium). Despite some variability the majority of cystic lesions in *Ptf1a-Cre; Kras^{G12D}; Brg1$^{f/f}$* mice presented with thin stroma lacking cells with wavy nuclei. (**b**) H&E staining of representative fibrovascular bundle in *Ptf1a-Cre; Kras^{G12D}; Brg1$^{f/f}$* pancreata. **(c)** Cystic lesions of *Ptf1a-Cre; Kras^{G12D}; Brg1$^{f/f}$* and PanINs of *Ptf1a-Cre; Kras^{G12D}* mice stain positive for Muc5AC (**a'-e'**), and Muc1 (**a'''-e'''**), but are negative for Muc2 (**a''-e''**). In contrast, ducts of control mice do not express Muc5AC and Muc2 (**a', a'', a'''**). The mucin expression pattern of the cystic lesions in *Ptf1a-Cre; Kras^{G12D}; Brg1$^{f/f}$* pancreata (positivity for Muc1, and Muc5AC and negativity for Muc2) matches that of human IPMNs of the pancreatobiliary type (**e', e'', e'''**). **(a)** and **(c)** scale bar 50μm, **(b)** scale bar 100μm.

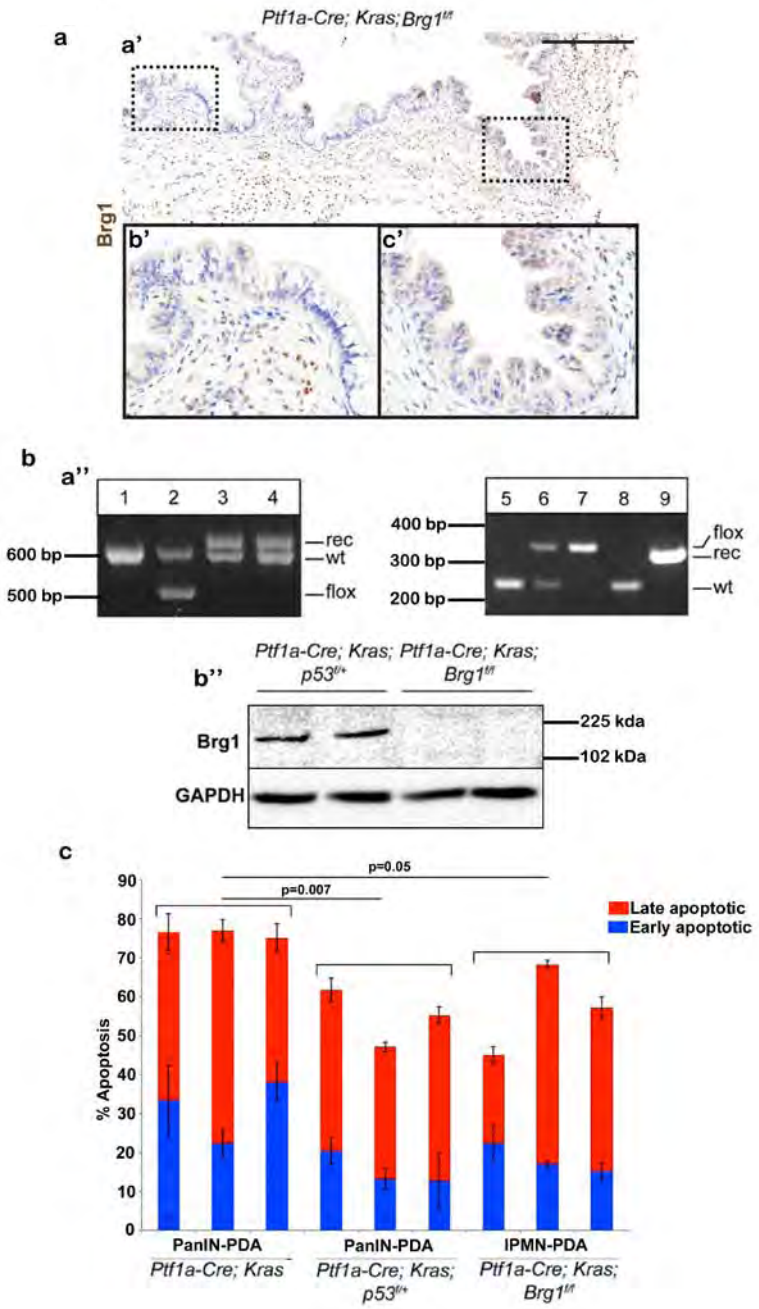

Supplementary Figure 2 Brg1 is lost in neoplastic epithelium of *Ptf1a-Cre; Kras^{G12D}; Brg1$^{f/f}$* mice and characterization of Brg1 null PDA cell lines. (**a**) (**a'**) Immunohistochemistry staining for Brg1 on neoplastic epithelium of a 9 weeks old *Ptf1a-Cre; Kras^{G12D}; Brg1$^{f/f}$* mouse. Low grade dysplasia marked by the presence of abundant mucin, undulating base, nuclear enlargement, or papillary or very dilated structures, tended to be negative for Brg1. In contrast, intermediate to high-grade dysplasia was uniformly negative for Brg1. (**b'**) Higher magnification of a low-grade dysplastic epithelium. (**c'**) Higher magnification of an intermediate to high-grade dysplastic epithelium. Scale bar 250µm. (**b**) **(a")** PCR analysis of the *Kras^{G12D}* (*Kras* PCR: 1-4) and *Brg1$^{f/f}$* (*Brg1* PCR: 5-9) alleles in cancer cell lines. Murine genomic DNA was isolated from the following sources 1: *Kras$^{+/+}$* (embryonic fibroblasts isolated from a wild type mouse). 2: unrecombined *Kras$^{G12D/+}$* (embryonic fibroblasts isolated from a *Kras$^{G12D/+}$* mouse). 3: *Ptf1a-Cre; Kras^{G12D}; p53$^{f/+}$* cancer cell line. 4: *Ptf1a-Cre; Kras^{G12D}; Brg1$^{f/f}$* cancer cell line. 5: Brg1$^{+/+}$ (tail of a wild type mouse). 6: unrecombined *Brg1$^{f/+}$* (tail of *Brg1$^{f/+}$* mouse). 7: unrecombined *Brg1$^{f/f}$* (tail of *Brg1$^{f/f}$* mouse). 8: *Ptf1a-Cre; Kras^{G12D}; p53$^{f/+}$* cancer cell line. 9: *Ptf1a-Cre; Kras^{G12D}; Brg1$^{f/f}$* cancer cell line. wt = wt allele, flox = unrecombined floxed allele, rec = recombined floxed allele. (**b"**) Western blot analysis of Brg1 in cancer cell lines derived from IPMN- and PanIN-PDAs. (**c**) Anoikis analysis of PanIN-PDA (n=3), IPMN-PDA (n=3 independent experiments) and *Ptf1a-Cre; Kras^{G12D}* (n=3 independent experiments) derived cancer cells by Annexin V/ PI staining. 200,000 Cells were seeded onto poly-hema coated petri dishes to inhibit cell adhesion. After 48 hours, detachment induced cell death or anoikis was assayed by measuring both early and late apoptosis. Total apoptosis is measured by counting both Annexin V single positive cells (early apoptotic) and Annexin V/ PI double positive cells are (late apoptotic). Values are shown mean +/- SD. p value for total apoptosis was calculated by one way ANOVA between three sets of cell lines.

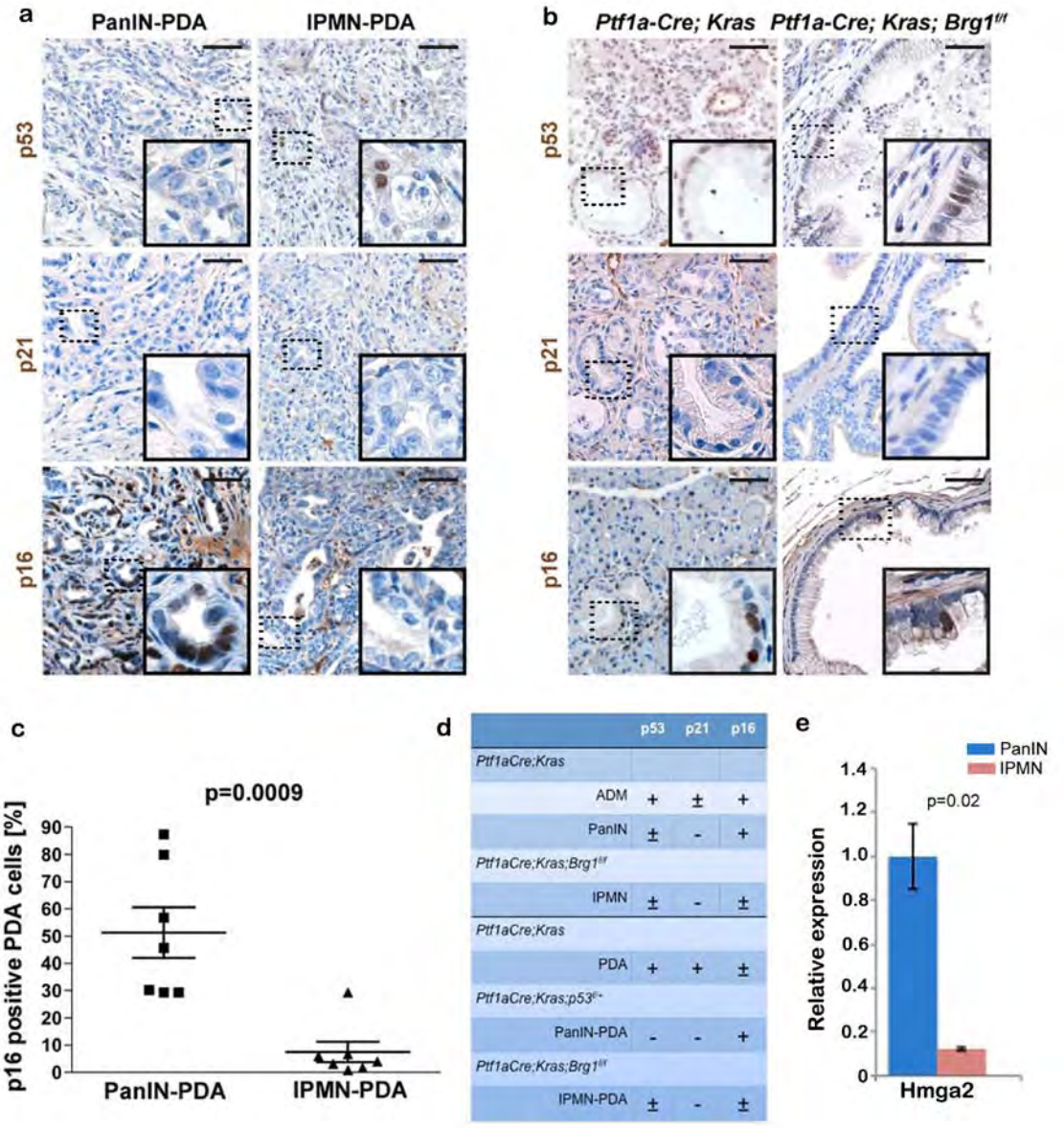

Supplementary Figure 3 Tumor suppressor gene expression in PDA and PDA precursor lesions. (**a**) Immunohistochemistry staining for p53, p21, and p16 on pancreatic tissue isolated from PanIN-PDA and IPMN-PDA in mice. Scale bars 50μm. (**b**) Immunohistochemistry for p53, p21, and p16 in ADM/PanIN and IPMN neoplastic precursor lesions on pancreatic sections derived from *Ptf1a-Cre; Kras^{G12D}* and *Ptf1a-Cre; Kras^{G12D}; Brg1$^{f/f}$* mice. Insets show higher magnification pictures of PanIN or IPMN lesions. Scale bars 50μm. (**c**) Quantification of p16 positive PDA cells in PanIN- vs. IPMN-PDA (n=7 tumours; values are shown as mean ± s.e.m. unpaired t-test was used for calculating p values). (**d**) Summary of tumor suppressor gene expression in cancer and precursor lesions of the respective genotypes. **(e)** Real-time PCR (RT-PCR) for Hmga2 relative to Cyclophilin A in murine pancreas containing PanIN (from *Ptf1a-Cre; Kras^{G12D}* mice; n=3) or IPMN (from *Ptf1a-Cre; Kras^{G12D}; Brg1$^{f/f}$* mice; n=3) lesions. Values are shown mean ± s.e.m. Unpaired t-test was performed to calculate the p value.

a

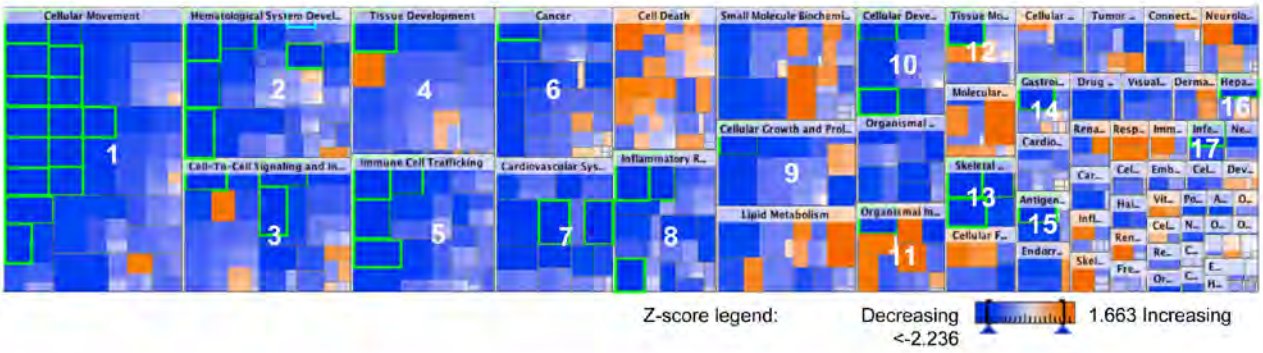

b

Category	Functions Annotation	p-Value	Predicted Activation State	Activation z-score
Cellular Movement	cell movement	5.15E-14	Decreased	-2.896
Cellular Movement	invasion of tumor cell lines	1.02E-13	Decreased	-2.862
Cellular Movement	cell movement of muscle cells	4.69E-04	Decreased	-2.818
Cellular Movement	migration of cells	2.32E-13	Decreased	-2.697
Cellular Movement	migration of muscle cells	2.03E-04	Decreased	-2.655
Cellular Movement	cell movement of phagocytes	3.66E-11	Decreased	-2.590
Cellular Movement	migration of smooth muscle cells	1.26E-04	Decreased	-2.468
Cardiovascular System Development and Function	angiogenesis of tumor	3.72E-04	Decreased	-2.395
Cellular Movement	cell movement of myeloid cells	4.23E-09	Decreased	-2.395
Cell-To-Cell Signaling and Interaction	binding of breast cancer cell lines	1.65E-04	Decreased	-2.392
Cancer	metastasis	3.07E-15	Decreased	-2.358
Cellular Growth and Proliferation	proliferation of smooth muscle cells	4.60E-04	Decreased	-2.262
Cell-To-Cell Signaling and Interaction	binding of tumor cell lines	5.73E-05	Decreased	-2.206
Tissue Development	adhesion of connective tissue cells	6.95E-05	Decreased	-2.203
Cellular Movement	migration of endothelial cells	2.40E-04	Decreased	-2.201

Supplementary Figure 4 Brg1 null PDA cells display a gene pathway signature indicative of lower malignant potential. Gene pathway/function analysis displaying the deep sequencing results of PanIN-PDA versus Brg1 null IPMN-PDA using Ingenuity® software. The analysis was performed by focusing on those genes with significantly altered expression levels ($p<0.05$) between PanIN- and IPMN-PDA. (**a**) Depicted is the heatmap clustering of the affected genes grouped into categories of cellular function. Highlighted in green are gene signatures with a z-score <=-2. The z-score reflects the significance and direction of the deviation of the individual gene signature from the mean. Category 1=Cellular Movement, 2=Hematological System Development and function, 3=Cell to cell signaling and interaction, 4=Tissue Development, 5=Immune Cell Trafficking, 6=Cancer, 7=Cardiovascular system development and function, 8=Inflammatory response, 9=Cellular growth and proliferation, 10=Cellular development, 11=Organismal injury and abnormalities, 12=Tissue morphology, 13=Skeletal and muscular system development and function, 14=Gastrointestinal diseases, 15=Antigen presentation, 16=Hepatic system disease, 17=Infectious disease. (**b**) List of the 15 most significantly down-regulated pathways in IPMN-PDA.

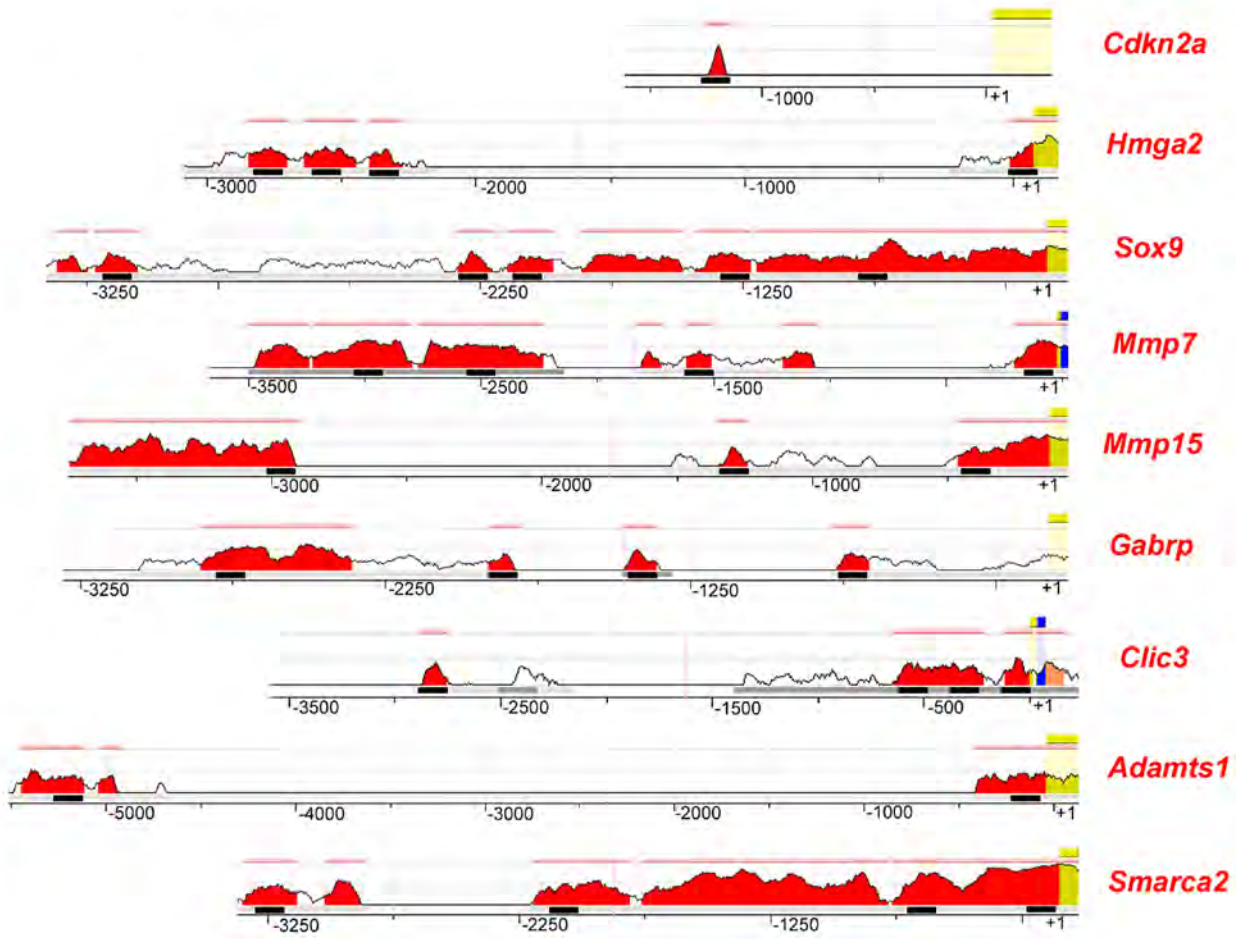

Supplementary Figure 5 Sequence alignment of promoter regions. Sequence alignment of promoter regions from mouse and human. Peak heights indicate degree of homology. Pink horizontal lines indicate evolutionary conserved regions. "+1" indicates the start site. Black boxes are regions analyzed by ChIP. Blue: Coding exons, Yellow: Untranslated region, Red: Promoter elements, Salmon: Intronic region.

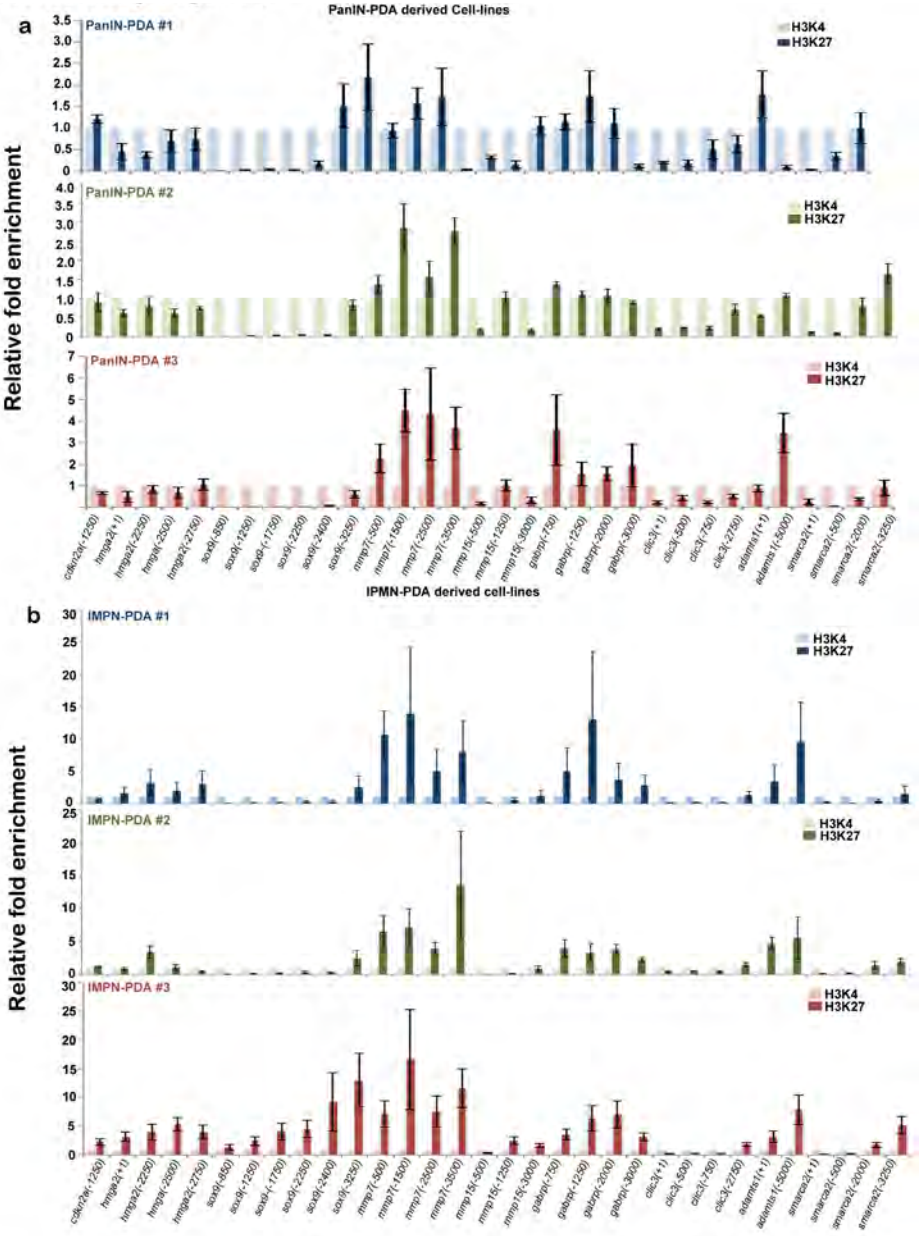

Supplementary Figure 6 ChIP analysis of promoter regions in PanIN- and IPMN-PDA cells. **(a)** Relative fold enrichment of H3K4Me3 and H3K27Me3 (over IgG control) on promoter regions in PanIN-PDA cells (1X10^6 cells/ ChIP, n=3 independent experiments). Decreases in the solid color bars (H3K27) indicate a relative increase in active chromatin marks. Increases in the solid bars point to a relative increase in repressive marks. Each panel indicates individual cell lines. Values are shown as mean ± s.e.m. **(b)** Relative fold enrichment of H3K4Me3 and H3K27Me3 (over IgG control) on promoter regions in IPMN-PDA cells (1X10^6 cells/ ChIP; n=3 independent experiments). Decreases in the solid color bars (H3K27) indicate a relative increase in active chromatin marks. Increases in the solid bars point to a relative increase in repressive marks. Each panel indicates individual cell lines. Values are shown as mean ± s.e.m.

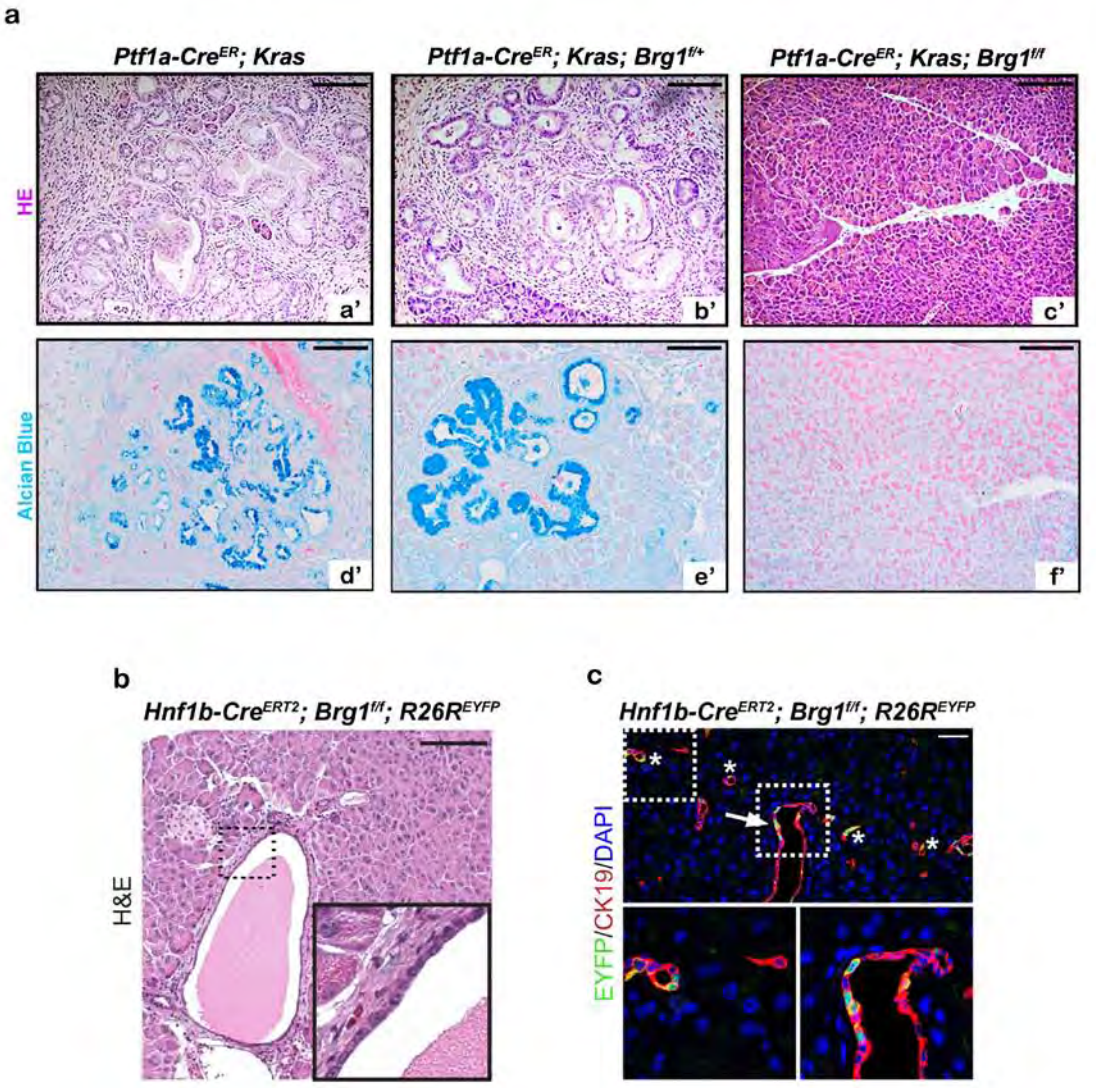

Supplementary Figure 7 Brg1 ablation abrogates PanIN formation from adult acinar cells and does not induce duct cell atypia in the absence of oncogenic Kras. **(a)** H&E and Alcian blue stainings of pancreata derived from *Ptf1a-Cre^{ER}; Kras* , *Ptf1a-Cre^{ER}; Kras; Brg1$^{f/+}$* (=Brg1 het) and *Ptf1a-Cre^{ER}; Kras; Brg1$^{f/f}$* (=Brg1 KO) mice 4 months after tamoxifen induction. Note the strong reduction of Alcian blue PanIN lesions in *Ptf1a-Cre^{ER}; Kras; Brg1$^{f/f}$* (=Brg1 KO) mice. (**b**) A representative image of a pancreatic duct of an *Hnf1b-Cre^{ERT2}; Brg1$^{f/f}$; R26R^{EYFP}* mouse 6 weeks after tamoxifen induction. A total of, 3 *Hnf1b-Cre^{ERT2}; Brg1$^{f/f}$* (± *R26R^{EYFP}*) mice were analyzed 6 weeks (n=1) or 12 weeks (n=2) after tamoxifen induction. None of the mice showed duct cell atypia on histological examination (**c**) YFP staining confirmed recombination upon tamoxifen administration in both the large (arrow) and small (asterisks) duct system. **(a)** and (**b**) Scale bar 100μm, (**c**) scale bar 50μm.

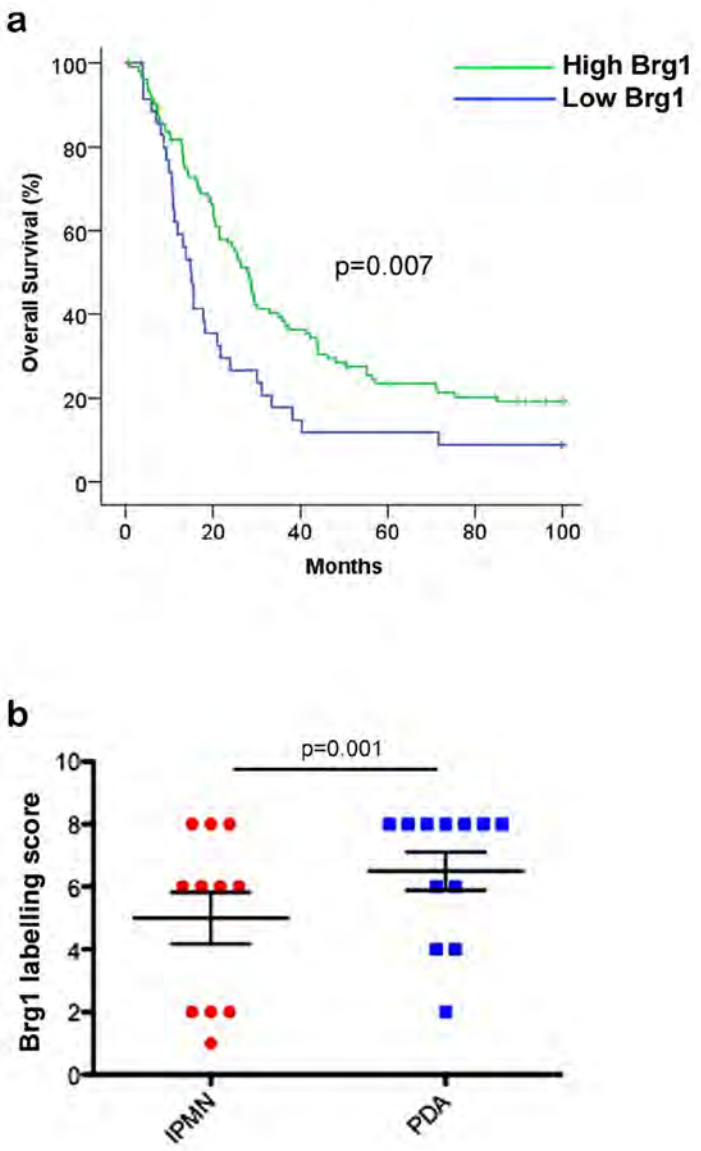

Supplementary Figure 8 Brg1 expression is associated with progression of human PanIN- and IPMN-PDA. (**a**) Kaplan-Meier survival curve of PanIN-PDA patients with low or high Brg1 expression in tumor cells (n=36 for low Brg1 and n=106 for high Brg1). Brg1 expression was scored using a histoscore ranging from 0-8 (low to high expression). The cut off histoscore was 0-6 for low and 7-8 for high Brg1 expression. Log rank test, p=0.007. Median survival was for low BRG1 = 15.1 months (95% CI 12.3-18.0) and for high BRG1 = 28.1 months (95% CI 24.3-31.8). (**b**) Brg1 labeling score from matched patient samples with IPMN and associated IPMN-PDA. The Brg1 expression was scored on the same section of a patient sample that contained an IPMN precursor and its associated IPMN-PDA. p value was calculated using the paired t-test; n=11 samples for IPMN precursors and n=12 samples for IPMN-PDA, values are shown as mean ± s.e.m.

Supplementary Information: DNA/ protein Gels

related to Supplementary Fig. 2b:
Kras recombination

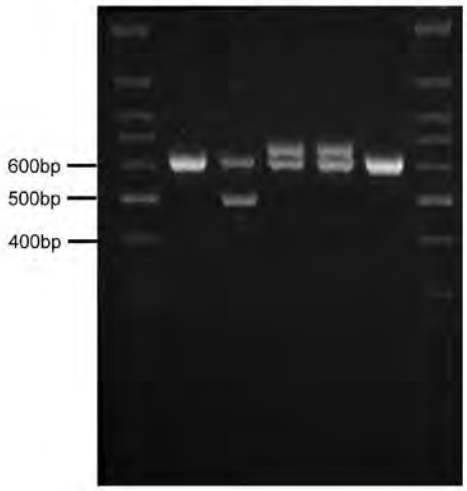

related to Supplementary Fig. 2b:
Brg1 recombination

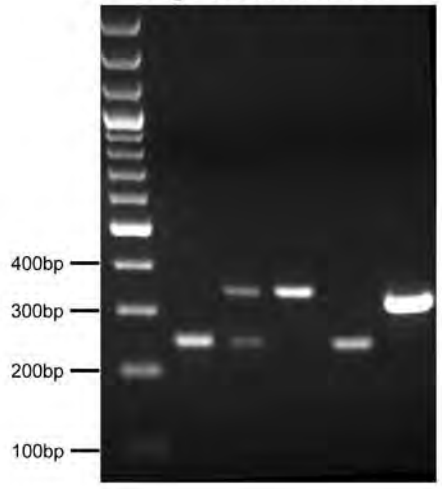

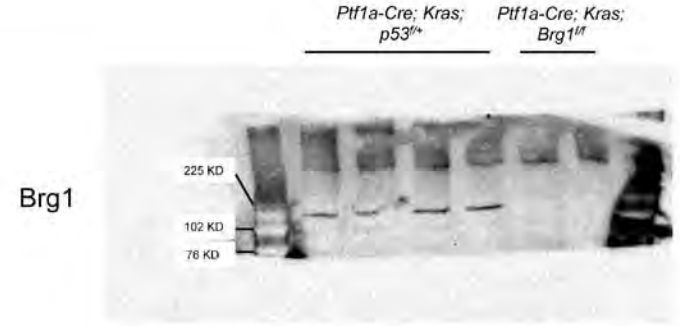

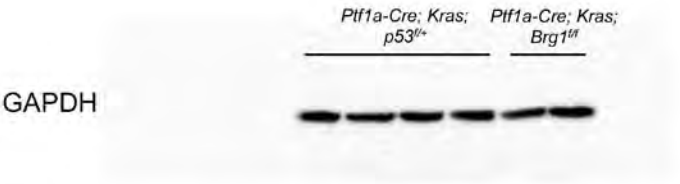

For GAPDH, the membrane was cut just below 52KD.

Supplementary Figure 9 DNA/protein gels

Supplementary Tables

Supplementary Table 1: Detailed analysis of disease spectrum at necropsy
Necropsy findings of mice of the indicated cohorts and age that died spontaneously or had to be sacrificed because of severe illness.

Supplementary Table 2: Deep Sequencing analysis of subcutaneous tumor RNA of IPMN-PDA vs. PanIN-PDA cancer cell lines
Depicted are all the statistically significant differentially expressed genes (1210 out of 29864 genes) by RNA deep sequencing analysis in IPMN-PDAs compared to PanIN-PDAs. p value (Actb) <0.05 was considered to be significant.

Supplementary Table 3: Increased and decreased gene function categories in Brg1 null PDA cells
The analysis was performed using Ingenuity® in analogy to Supplementary Figure 8. Genes from the RNA deep sequencing analysis that were significantly different (p value (Actb) < 0.05) between PanIN- and IPMN-PDA cells were included. Depicted are all gene function categories with a z-score ≤ 2 or ≥ 2. Redundant gene function categories are not shown.